The Armed Forces Institute of Pathology
Department of Veterinary Pathology

Conference Coordinator
Matthew Wegner, DVM
Major, Veterinary Corps, U.S. Army
Department of Veterinary Pathology
Armed Forces Institute of Pathology
Registry of Veterinary Pathology

WEDNESDAY SLIDE CONFERENCE 2010-2011

Conference 9

20 October 2010

Conference Moderator:
Brett Saladino, DVM, MBA, Diplomate ACVP
Associate Director of Pathology
Covance Laboratories, Inc.
Madison, WI

CASE I: AFIP 3 (AFIP 3152405).

Signalment: 70-week-old, male, Wistar-Han, rat (*Rattus norvegicus*).

History: Tissue from the thoracic cavity of a control group male rat on a two year carcinogenicity study.

Gross Pathology: The thoracic cavity contained a 3 x 3 x 2 cm, tan, multilobular mediastinal mass.

Laboratory Results: Immunohistochemical stain: immunolabeling for UCP-1 (uncoupling protein 1). Transmission electron microscopy: numerous mitochondria with transverse cristae.

Histopathologic Description: Fibroadipose tissue: Tissue consists of lobules of neoplastic cells separated by irregular thin to broad trabeculae of fibrous connective tissue. Neoplastic cells are polyhedral with homogeneous eosinophilic to microvacuolated cytoplasm and nuclei are round to oval with stippled chromatin and 0-2 nucleoli. Mitoses are 0-1/HPF. These cells are frequently admixed with unilocular adipocytes that have eccentric nuclei. There is marked anisocytosis and anisokaryosis, and there are scattered karyomegalic cells. There are multiple foci of coagulative necrosis sometimes surrounded by foamy macrophages and multinucleate giant cells, and occasional lakes of proteinaceous fluid containing foamy macrophages. In some sections, connective tissue trabeculae contain hemorrhage and loose aggregates of pigmented macrophages (hemosiderophages), plasma cells, and lymphocytes.

Contributor's Morphologic Diagnosis: Hibernoma, malignant.

Contributor's Comment: Hibernomas are rare, well-characterized neoplasms of brown adipose tissue (BAT) in humans and animals. Historically, the background incidence has been low in rodent carcinogenicity studies. This tissue was from a two year study, in group-housed male and female Wistar-Han rats, with an unusually high incidence of non-test article-related hibernomas (up to 12% in control animals).[3] For an unknown reason, the incidence was higher in males. For males and females, the majority of hibernomas were noted in the thoracic cavity as tan to red lobulated masses. Larger tumors had necrotic foci bordered by granulomatous inflammation. Tumor emboli were present in vascular lumina as well as in the lungs. Characteristic ultrastructural features were abundant mitochondria with parallel lamellar cristae and variably sized lipid droplets. Immunohistochemically, neoplastic cells stained positively for UCP1 (uncoupling protein 1), generally considered a specific marker of brown adipocytes. Although stimulation and regression of BAT secondary to changes in the ambient environment as well as chronic disease states is reported,[7] a high incidence of spontaneous hibernomas occurred in this study. Hibernomas were not observed in the concurrent mouse carcinogenicity study with the same test article

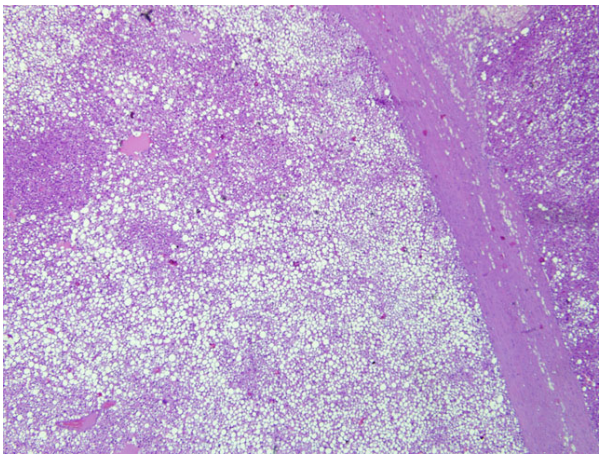

1-1. Fibroadipose tissue, Wistar-Han rat. The multilobulated neoplasm is divided by variably dense bands of fibrous connective tissue and composed of large, vacuolated polygonal cells. (HE 40X)

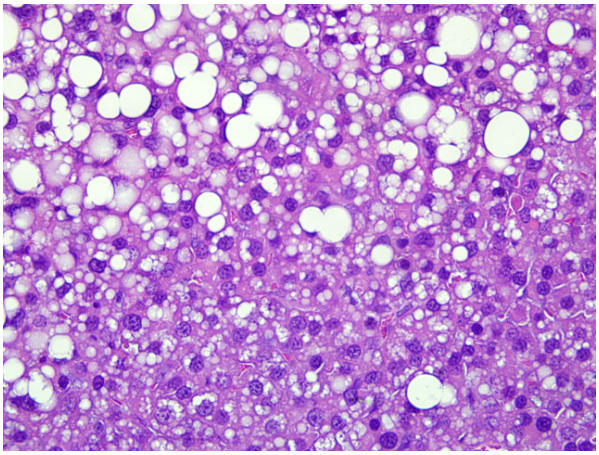

1-2. Fibroadipose tissue, Wistar-Han rat. Neoplastic cells have vacuolated cytoplasm and round to oval nuclei with finely stippled chromatin. Neoplastic cells are often admixed with unilocular adipocytes that have an eccentric nucleus. (HE 400X)

conducted at the same laboratory.[3] Although hyperplasia and/or neoplasia of BAT have been observed with several classes of unrelated pharmaceutical compounds,[1,6,7] the historical incidence of spontaneous hibernomas in rats has been very low. Increased incidences of spontaneous hibernomas unrelated to the administration of test articles were also observed in Sprague-Dawley rats in three different carcinogenesis bioassays conducted during approximately the same time period.[2]

The primary function of brown adipose tissue is to provide nonshivering thermogenesis during periods of cold-induced stress. Brown adipose tissue is considered especially critical in neonates, in which deposits are within abdominal and thoracic cavities as well as in subcutaneous tissue of the interscapular region. In rodents, BAT deposits normally persist in multiple locations throughout life. Brown adipose cells, packed with mitochondria, are specialized for thermogenesis.[4] Cold stress induces the release of norepinephrine, which binds to β-adrenergic receptors on brown adipocytes.[2] This binding activates lipoprotein lipase to liberate free fatty acids, and initiates the adenylcyclase-cAMP-lipase activation signal that stimulates β–oxidation of fatty acids in mitochondria.[4] Free fatty acids act as ionophore uncouplers in BAT mitochondria. UCP-1, localized to the inner mitochondrial membrane, uncouples fatty acid oxidation from ADP phosphorylation and promotes the dissipation of the energy generated by oxidation as heat.[2]

AFIP Diagnosis: Fibroadipose tissue: Hibernoma.

Conference Comment: Participants generally agreed with the diagnosis of hibernoma for the lesion. With no discernable normal tissue, features of malignancy, such as stromal invasion, evidence of metastasis or tumor emboli within lymphatics or vasculature, cannot be adequately assessed. After the moderator provided additional information from the contributor during the conference, a diagnosis of malignant hibernoma is appropriate.

Historically, the literature refers to benign tumors of brown adipose tissue as hibernomas while classifying malignant tumors of brown adipose tissue liposarcomas.[5] Utilizing immunohistochemical and ultrastructural examination, closer investigation of tumors of brown adipose tissue supports a diagnosis of malignant hibernoma rather than liposarcoma.[2,3] This raises the possibility that malignant hibernomas previously have been misdiagnosed/misclassified and are therefore more common than previous data suggest. This presents a problem from a toxicologic pathology standpoint in that historical data may be skewed. It is therefore difficult to discern whether malignant hibernomas are test-article related or are spontaneous occurrences in certain strains of rats.

The contributor provides an excellent overview of the function and physiology of brown adipose tissue.

Contributor: Covance Laboratories, Inc, Madison, Wisconsin, USA.
www.covance.com

References:

1. Brees DJ, Elwell MR, Tingley FD, et al. Pharmacological effects of nicotine on norepinephrine metabolism in rat brown adipose tissue: relevance to nicotinic therapies for smoking cessation. *Toxicol Pathol*. 2008;36:568-575.

2. Bruner RH, Novilla MN, Picut CA, et al. Spontaneous hibernomas in Sprague-Dawley rats. *Toxicol Pathol*. 2009;37:547-552.
3. Chandra S, Dochterman W, Ploch S, et al. A carcinogenicity study with unusually high incidence of spontaneous hibernomas in Wistar-Han rats. *Toxicol Pathol*. 2009;37:127(P14).
4. Cheville NF. An introduction to interpretation In: *Ultrastructural Pathology*. Ames, IA: Iowa State University Press; 1994:14.
5. Greaves P, Faccini JM, Courtney CL. Proliferative lesions of soft tissues and skeletal muscles in rats, MST-1. In: *Guides for Toxicologic Pathology*. Washington, DC: STP/ARP/AFIP; 1992:3.
6. Herman JR, Dethloff LA, McGuire EJ, et al. Rodent carcinogenicity with the thiazolidinedione antidiabetic agent troglitazone. *Toxicol Sci*. 2002;68:226-236.
7. Poulet FM, Berardi MR, Halliwell W, Hartman B, Auletta C, Bolte H. Development of hibernomas in rats dosed with phentolamine mesylate during the 24-month carcinogenicity study. *Toxicol Pathol*. 2004;32:558-566.

CASE II: PFIZER SND CASE 2 (AFIP 3164224).

Signalment: Mature, male, Wistar-Han, rat (*Rattus norvegicus*).

History: This rat was part of an exploratory toxicity study; it was approximately eight weeks old at study initiation. The rat was administered a once weekly intravenous bolus of doxorubicin (3 mg/kg) for 6 weeks and was found dead on study day 52, a few hours before the scheduled euthanasia/necropsy.

Gross Pathology: Macroscopic findings in these animals included small testes and epididymides which correlated with marked to severe degeneration of the seminiferous tubules and epididymal oligospermia histologically. Some animals were also observed to have a gelatinous edematous pancreas.

Histopathologic Description: Heart: Within the heart there is severe cardiomyocyte degeneration in the left atrium with marked vacuolation, and lesser myofiber disorganization, fragmentation and hypereosinophilia. Rarely, myofiber necrosis is present, with necrotic myocytes exhibiting apoptotic or karyorrhectic nuclei. Vessels within the left atrium have plump reactive endothelium and contain marginating neutrophils. A 4-6 mm diameter laminated fibrin thrombus distends the left atrium and is multifocally adherent to the endocardium. The margin of the thrombus contains numerous degenerate and viable neutrophils, and abundant apoptotic debris. Depending on the section, rare to large colonies of 1-2 µm bacterial coccobacilli are noted within the thrombus, extracellularly or phagocytosed by leukocytes. The left atrial endocardial endothelium is plump and reactive, multifocally eroded, and the endocardium is expanded by transmigrating neutrophils. Additionally, there is minimal to mild cardiac myofiber degeneration with myofiber vacuolation and myofibrillar disorganization within the septum, left ventricle and right atrium.

Additional histologic lesions in these rats referable to doxorubicin administration are present in the kidneys, testes, epididymides and lungs. Kidney lesions included tubular degeneration/ regeneration, glomerular atrophy and vacuolation and hyperplasia/ hypertrophy of Bowman's capsule. Testicular lesions consisted of germ cell loss, with only Sertoli cells remaining within seminiferous tubules in severe cases. A secondary oligospermia was present within the epididymides. Within the lung there was degeneration, with prominent vacuolation, of the muscular media in

2-1. Heart, Wistar-Han rat. There is diffuse cardiomyocyte vacuolation, degeneration, necrosis, and loss in the left atrial wall. The left atrium is dilated and partially filled by a large thrombus adhered to the endocardium. (HE 40X)

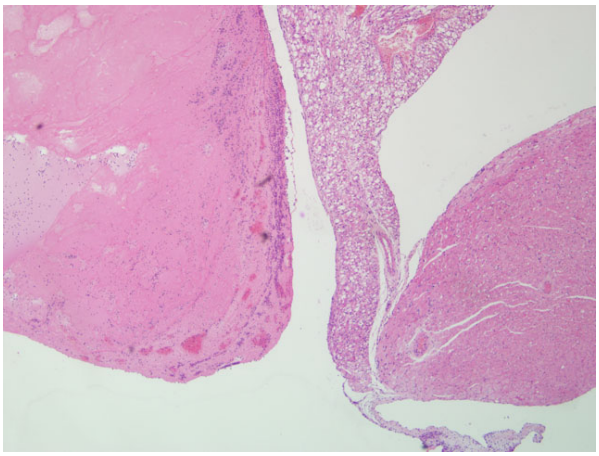

2-2. Heart, atria, Wistar-Han rat. Endothelial cells in vessels of the left are hypertrophied , reactive, and multifocally eroded and transmigrated by moderate numbers of neutrophils. (HE 400X)

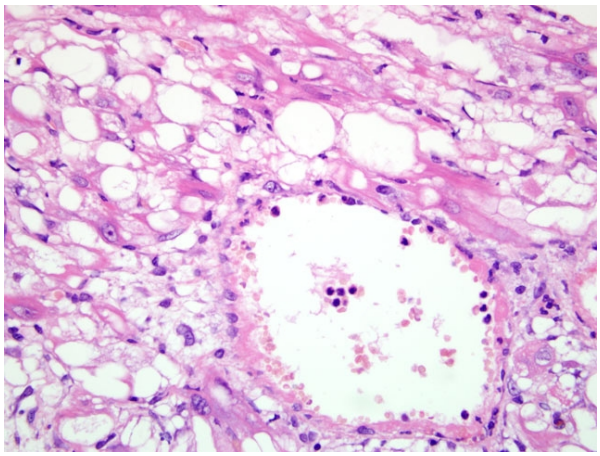

large arteries, sometimes accompanied by inflammation and fibrinoid necrosis.

Contributor's Morphologic Diagnosis: 1. Heart: Multifocal cardiac myocyte degeneration with prominent vacuolation, and rare necrosis.
2. Heart, left atrium: Atrial thrombosis and neutrophilic endocarditis, with intralesional bacteria.

Contributor's Comment: Doxorubicin (adriamycin) is an anti-cancer drug with a very wide antitumor spectrum, and efficacy against both solid tumors and haematological malignancies.[2,5] However, use of the drug is limited by the frequent occurrence of dose-dependent cardiotoxicity which produces cardiomyopathy and secondary congestive heart failure.[2] Acute doxorubicin toxicity in patients includes gastrointestinal complaints, cardiac arrhythmias, phlebitis and tissue necrosis from paravasal leakage, and hypersensitivity reactions.[5] Delayed toxicity includes myelosuppression, alopecia and cardiomyopathy, with chronic cardiotoxicity manifesting as congestive heart failure.[5] Doxorubicin has been used for nearly three decades as a chemotherapeutic, but only recently have some of the cytotoxic mechanisms of the drug been elucidated.[5] These include free radical formation, membrane lipid peroxidation, iron-dependent oxidative damage to macromolecules, direct DNA damage or interference with DNA repair, mitochondrial damage and induction of immune reactions involving antigen-presenting cells in the heart.[1,2] Free radical formation and redox cycling associated with doxorubicin treatment cause the generation of reactive oxygen species such as superoxide anion, hydrogen peroxide and hydroxyl radical.[2] Tissues with a less developed antioxidant defense mechanism, like the heart, are highly susceptible to anthracycline-induced oxygen radicals.[2]

The doxorubicin-induced lesions in this study increased in incidence and/or severity with increasing duration of dosing. Both the cumulative effect and the morphologic characteristics of the lesions were consistent with findings reported in the literature. The myocardial degeneration induced in the ventricles and septum in this study in rats was representative of that reported in mice in the literature; however, atrial lesions were much more severe. A similar pattern was described previously in mice treated with doxorubicin,[3] although the bulk of the literature describing heart lesions caused by doxorubicin is based on examination of transverse tissue sections taken through the mid-ventricular and septal areas, which do not include evaluation of the atria. In mice, vacuolation and degeneration of atrial myocytes are shown with electron microscopy to be dilation of the sarcoplasmic reticulum and increased numbers of normal and/or degenerate mitochondria.[3] Atrial interstitial inflammatory cell infiltrates within the myocardium and endocardium are also reported.[3] Additionally, mice treated with doxorubicin show an incidence of atrial thrombosis approaching 75%.[3] The proposed cause of the atrial thrombosis in the mice was endothelial inflammation accompanied by abnormal blood flow secondary to the myocardial damage.[3]

AFIP Diagnosis: Heart, atria: Cardiomyocyte vacuolar degeneration, necrosis and loss, diffuse, mild to severe with left atrial thrombosis and rare regeneration.

Conference Comment: The contributor provides an excellent review of doxorubicin toxicity. The moderator highlighted the point that the contributor makes above; that is, although doxorubicin toxicity is traditionally associated with ventricular, rather than atrial, cardiomyocyte vacuolization and degeneration, this is related to tissue sample sectioning rather than to a change in pathologic mechanism of doxorubicin. The atrial lesions in previous studies likely were not noted earlier because the atria were not sectioned for histopathologic examination. This underscores the complexity of toxicologic pathology and the importance of being thorough in toxicity studies. This case also represents a paradigm shift in how some participants evaluate and interpret the tissue changes, i.e. they initially speculated that doxorubicin could cause this type of lesion in the heart, but then discounted it as the etiology because the lesion is observed in the atrium rather than the ventricle. Lack of awareness that doxorubricin could induce lesions in the cardiac atria caused several participants to dismiss it as a possible etiology in favor of other toxic causes, thus illustrating the informational utility of this case.

Discussion then focused on the secondary effects of the histologic lesions in the atria. Residents concluded that the primary lesion is the myocardial change, which results in ineffective myocardial contraction, endothelial damage, release of prothrombotic substances and thrombosis. Three perturbations promoting thrombus formation, colloquially referred to as Virchow's triad, are endothelial injury, altered normal blood flow (turbulence or stasis), and hypercoagulability.[4] Endothelial cell damage is not restricted to physical damage; any damage capable of disrupting the prothrombotic-antithrombotic balance favoring thrombosis is included in this category.[4]

Normal, non-activated endothelial cells have antithrombotic activity; activation or damage resulting from bacterial endotoxin, cytokines or changes in hemodynamic properties promote thrombus formation. The chart on the following page summarizes the mechanisms for these actions.[4]

Antithrombotic Properties of Endothelial Cells		Prothrombotic Properties of Endothelial Cells	
Antiplatelet effects	• Covers thrombogenic subendothelial extracellular matrix (ECM) • Produce PGI_2 and nitric oxide inhibiting adhesion • Produces adenosine diphosphatase to degrade ADP	Platelet effects	• Endothelial injury exposes subendothelial ECM → platelet adherence via von Willebrand factor
Anticoagulant effects	•Heparin-like molecules enhance thrombin inactivation via antithrombin III: 1. Thrombomodulin → binds thrombin → activates protein C → inactivates factors Va and VIIIa → inhibits clotting 2. Produces protein S and tissue factor pathway inhibitor → direct inhibition of factor VIIa (tissue factor) and factor Xa	Procoagulant effects	•Cytokine (TNF or IL-1) or endotoxin → endothelial production of tissue factor → activation of the extrinsic clotting cascade Augment the catalytic function of activated factor IXa and Xa
Fibrinolytic effects	Produce tissue plasminogen activator → cleaves plasminogen to plasmin → cleaves fibrin → thrombus dissolution	Antifibrinolytic effects	Secrete inhibitors of plasminogen activator → reduces fibrinolysis

Platelets play an equally important role in hemostasis. Once contact is made with extracellular matric (ECM) proteins, platelets have three functions:[4]

1. Adhere to collagen with glycoprotein Ib via vWF; additional glycoprotein receptors bind other ECM components.
2. Secretion of α- and dense-granule contents promoting thrombus formation. P-selectin-coated α-granules contain fibrinogen, fibronectin, platelet factor 4, PDGF, TGF-β, and factors V and VIII. Dense (δ) granules have ionized calcium, histamine, serotonin, epinephrine, ADP and ATP.
3. Platelets aggregate and change shape, forming the primary hemostatic plug.

The severity modifier in our morphologic diagnosis is intended to indicate that the lesion in the right atrium is mild, while the lesion in the left atrium is severe. There is likely some sectioning variability as participants did not see the bacteria described by the contributor.

Contributor: Pfizer Global Research and Development, Sandwich Laboratories, Sandwich, Kent, United Kingdom.

References:

1. Arola OJ, Saraste A, Pulkki K, Kallajoki M, Parvinen M, Voipio-Pulkki LM. Acute doxorubicin cardiotoxicity involves cardiomyocyte apoptosis. *Cancer Res*. 2000;60:1789-1792.

2. Ayaz SA, Bhandari U, Pillai KK. Influence of DL α-lipoic acid and vitamin-E against doxorubicin-induced biochemical and histological changes in the cardiac tissue of rats. *Indian J Pharmacol*. 2005;37(5): 294-299.

3. Fujihira S, Yamamoto T, Matsumoto M, et al. The high incidence of atrial thrombosis in mice given doxorubicin. *Tox Pathol*. 1993;21(4):362-368.

4. Mitchell RN. Hemodynamic disorders, thromboembolic disease and shock. In: Kumar V, Abbas AK, Fausto N, Aster JC eds. *Robbins and Cotran Pathologic Basis of Disease*. 8th ed. Philadelphia, PA: Elsevier Saunders; 2009:115-123.

5. Speth PAJ, van Hoesel Q, Haanen C. Clinical pharmacokinetics of doxorubicin. *Clin Pharm*. 1988;15:15-31.

CASE III: 10-016 (AFIP 3168181).

Signalment: 11 to 12-month-old, male and female, Balb/c transgenic mice (HSP70, TLR2) (*Mus musculus*).

History: Three Balb/c mice weighing about 35 gm were submitted with a large submandibular swelling.

Gross Pathology: Incision of the skin in the submandibular region revealed a large, smooth, soft, round, blood-filled, multi-lobulated mass measuring about 1.5 to 2 cm in diameter.

Histopathologic Description: Salivary gland: Expanding and infiltrating the salivary gland (submandibular, parotid or sublingual gland, varying depending on mouse and section), there is a large, variably encapsulated mass with multiple large cystic spaces filled with pale eosinophilic mucinous material and blood. Multifocally, irregular, variably-sized necrotic areas may be filled with amorphous eosinophilic cellular debris intermixed with pyknotic nuclear debris, or may form pseudocysts with no lining epithelium. Adjacent to blood vessels, the neoplastic cells tend to form palisades and have a predominant epithelioid morphology. The mass consists of variably distinct foci composed of spindle cell and polygonal epithelioid cell populations. The neoplastic spindloid cells have scant to moderate amounts of pale eosinophilic fibrillar cytoplasm and vesicular nuclei with 1-2 distinct nucleoli. There is moderate to marked nuclear atypia and numerous mitoses. The epithelioid cells have abundant pale eosinophilic fibrillar cytoplasm and round to oval basophilic stippled nuclei. There are rare misshaped and attenuated ducts and tubules entrapped within the neoplastic cell population, especially at the periphery of the mass. In addition, there are multifocal lymphoid cell infiltrates near the periphery of the neoplasm. Surrounding the neoplastic tissue, there are multifocal areas of a variable amount of granulation tissue intermixed with hemorrhage and inflammatory cells (neutrophils and large foamy macrophages) that often extends into the dermis.

Contributor's Morphologic Diagnosis: Salivary gland: Myoepithelioma.

Contributor's Comment: These are very rare neoplasms seen most commonly in BALB/c, A, C58 strains. [3,5] Clinically, the neoplasm presents as fluctuant swelling in the ventral aspect of the neck. Macroscopically, the neoplasms are dark red to yellow, solid to cystic masses filled with mucus, blood and necrotic cellular debris. They are presumed to arise from the myoepithelial cells of the salivary glands (mainly parotid and submandibular and less commonly

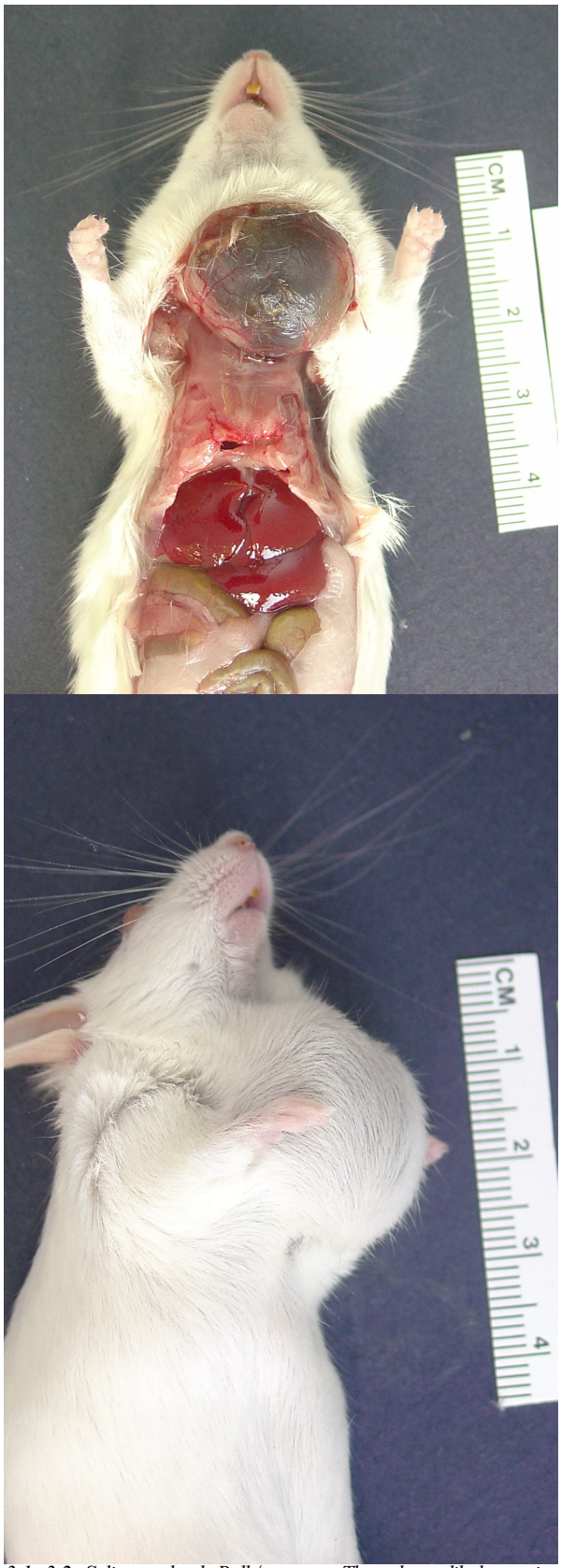

3-1, 3-2. Salivary gland, Balb/c mouse. The submandibular region contains a large, smooth, soft, round, blood filled multilobulated mass measuring about 1.5 to 2.0 cm in diameter. Photographs courtesy of Experimental Pathology Laboratories, Inc., PO Box 13566, Research Triangle Park, NC 27709, nallison@epl-inc.com

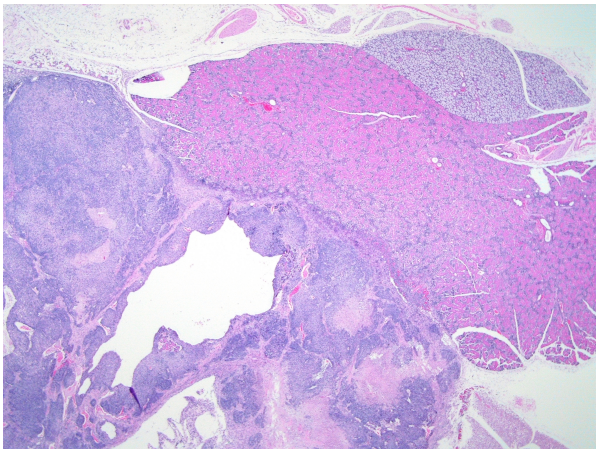

3-3. Salivary gland, Balb/c mouse. Expanding and infiltrating the salivary gland (parotid) is a large, variably encapsulated neoplasm with multiple, often blood filled cystic spaces. Photographs courtesy of Experimental Pathology Laboratories, Inc., PO Box 13566, Research Triangle Park, NC 27709, nallison@epl-inc.com

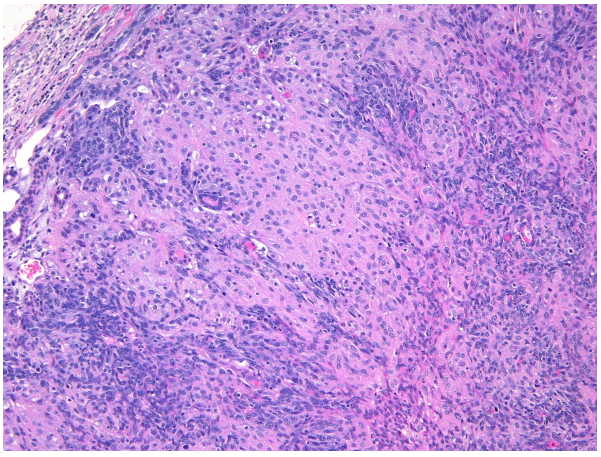

3-4, 3-5. Salivary gland, Balb/c mouse. The neoplasm is composed of both polygonal (large epithelioid) cells and spindle cells. Neoplastic spindle cells have scant to moderate amounts of pale eosinophilic cytoplasm and vesicular nuclei. The epithelioid cells have abundant pale eosinophilic fibrillar cytoplasm and round to oval basophilic stippled nuclei. Multifocally at the periphery of the neoplasm there are moderate numbers of lymphocytes. Photographs courtesy of Experimental Pathology Laboratories, Inc., PO Box 13566, Research Triangle Park, NC 27709, nallison@epl-inc.com

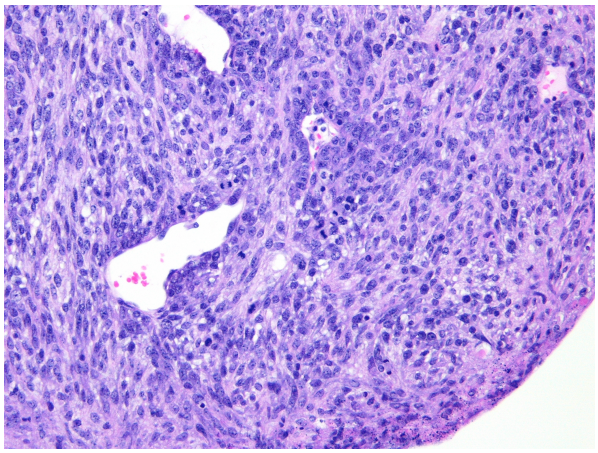

the sublingual gland). Histologically, these neoplasms are biphasic and are comprised of varying proportions of mesenchymal (spindle) cells and large epithelioid cells; either of these cell types may be the predominant population in a given tumor. Areas of degeneration and necrosis are relatively common. A majority of myoepitheliomas are circumscribed with a thin capsule and variable degree of invasion into adjacent tissues. However, metastasis to regional lymph nodes and lungs may be seen in rare cases.

The characteristic absence of formation of acini or ducts by the neoplastic cells aids in differentiating these tumors from adenomas and carcinomas. The presence of a single solitary mass on the ventral aspect of the neck helps to differentiate these neoplasms from polyoma virus-induced pleomorphic tumors that are multicentric in origin and not limited to the salivary glands.[3] Myoepitheliomas can also occur within mammary glands, Harderian glands, and clitoral glands and preputial glands.

In humans, salivary gland myoepitheliomas are classified based on morphology (plasmacytoid, spindle, stellate, clear or epithelioid) of the neoplastic cells into spindle cell myoepithelioma, clear cell myoepithelioma, etc. Due to the histologic heterogeneity, no single immunostain is diagnostic. For human salivary myoepitheliomas, a panel of markers consisting of AE1/AE3 (PAN-K), S-100, P63, GFAP, calponin and vimentin is commonly used for diagnosis.[4] A panel of markers, such as vimentin and cytokeratin (especially k5 and k14), may be used for immunohistochemical diagnosis of these tumors in mice. Also, PTAH staining will aid in confirmation of the presence of intracytoplasmic fibrils within the neoplastic epithelioid cells. Ultrastructurally, these fibrils are composed of abundant microfilaments in parallel orientation with periodic focal densities, characteristic of smooth muscle fibrils, and are arranged in dense parallel bundles around the nucleus.[3] These tumors are usually negative for smooth muscle actin and desmin.

Acknowledgements: We appreciate the help of Drs. Terry Blankenship-Paris, Mark Hoenerhoff, and Steven Kleeberger at NIEHS, RTP, NC for graciously sharing the case material.

AFIP Diagnosis: Salivary gland: Myoepithelioma, malignant.

Conference Comment: Conference participants agreed the histomorphologic features are consistent with the diagnosis of myoepithelioma. As indicated by the contributor, myoepitheliomas can have a diverse histomorphology. From personal experience, the moderator mentioned that the presence of spindle cells

which palisade around the outer edge of the tumor and forming a dark rim is a common histologic feature of the neoplasm. Additionally, neoplastic cells adjacent to vessels often take on an epithelial-type arrangement.[1] In addition to the features described by the contributor and the moderator, myoepithelioma also can occur histologically as a squamous form, both with keratin pearl formation or without the presence of keratinization.[1]

Participants discussed the differential diagnosis, which included poorly differentiated carcinoma/adenocarcinoma, carcinosarcoma, and sarcoma arising or metastatic to glandular organs, such as the salivary, mammary, lacrimal, and Harderian glands. All participants interpreted the tumor as arising from the salivary gland, and thus considered a neoplasm of other regional glandular tissues less likely, including mammary, lacrimal, or Harderian origin. Based on the absence of desmoplasia and glandular or squamous differentiation, participants considered a tumor of epithelial origin less likely; the glandular or ductular profiles occasionally found in the neoplasm were interpreted as preexisting salivary structures entrapped by neoplastic cells. Participants did observe the large pseudocystic structures in the neoplasm described by the contributor, which were not interpreted as evidence of glandular differentiation.

Finally, participants discussed the difficulty in the histologic differentiation of salivary myoepithelioma from polyoma virus-induced salivary neoplasms. Polyoma virus inoculated into neonatal mice of susceptible strains induces tumors in multiple organs, in particular the parotid salivary gland.[2] Histologically, polyoma virus-induced salivary neoplasia most commonly occurs as mixed mesenchymal and epithelioid populations, although neoplasms composed of pure mesenchymal or epithelioid populations may be observed.[2] In contrast to polyoma virus-induced salivary tumors, myoepitheliomas typically are not infiltrated by lymphocytes and plasma cells.[1]

The use of tissue from multiple animals in this case contributed to slide variation, with some slides having one type of salivary gland and others having more than one type present.

Contributor: Experimental Pathology Laboratories, Inc., PO Box 13566, Research Triangle Park, NC 27709
http://www.epl-inc.com

References:

1. Betton GR, Whiteley LO, Anver MR, et al. Gastrointestinal tract. In: Moore U, ed. *International Classification of Rodent Tumors: The Mouse*. Berlin, Germany: Springer-Verlag; 2001:29.
2. Botts S, Jokinen M, Gaillard ET, Elwell MR, Mann PC: Salivary, Harderian, and lacrimal gland glands. In: Maronpot RR, ed. Pathology of the Mouse. Vienna, IL: Cache Valley Press; 1999:56-60.
3. Burger GT, Frith CH, Townsend JW. Myoepithelioma, Salivary glands, mouse. In: Jones TC, Popp JA, Mohr U, eds. *Digestive system. Monographs on Pathology of Laboratory Animals*. Berlin, Germany: Springer-Verlag; 1997:231-235.
4. Hunt JL, Barnes L. Immunohistology of head and neck neoplasms. In: Dabbs D, ed. *Diagnostic Immunohistochemistry.* 2nd ed. Philadelphia, PA: Churchill Livingstone (Elsevier Inc.); 2006:245-247.
5. Sundberg JP, Hanson CA, Roop DR, Brown KS, Bedigian HG. Myoepitheliomas in inbred laboratory mice. *Vet Pathol*. 1991;28:313-323.

CASE IV: 10-4230 HE (AFIP 3170127).

Signalment: 9-year-old, female, spayed, German shepherd dog, canine (*Canis lupus familiaris*).

History: A 9-year-old, female spayed German Shepherd Dog presented to the referring veterinarian with a history of anorexia, vomiting and diarrhea of approximately 12 hours duration. A chemistry panel revealed a severely elevated ALT and low blood glucose. No abnormalities were noted on abdominal radiographs. The dog was treated with IV fluids and anti-emetics for a brief period of time, but developed seizures, at which point the owners elected to euthanize the dog.

Gross Pathology: (per RDVM history): The liver contained generalized multifocal pinpoint raised yellow areas. The stomach contents consisted of dark ingesta with hemorrhage. Scattered petechiae were noted within the pancreas. The abdominal and subcuticular adipose was diffusely yellow (jaundice).

Histopathologic Description: Liver: Severe diffuse loss of hepatocytes characterizes the section. Remaining hepatocytes are discohesive with pyknotic or karyolytic nuclei, with either micro-vacuolated (lipidosis, probable) or condensed and hypereosinophilic cytoplasm (necrosis). Confluent areas of hemorrhage, along with hemosiderin-laden macrophages fill spaces left by hepatocyte loss. On this background of necrosis and hemorrhage there are ribbons of preserved bile ducts, scattered foci of erythroid precursors (extramedullary hematopoiesis), and focal islands of plump, basophilic, often binucleate hepatocytes (regenerative nodules). Some centrilobular hepatocytes remain and are arranged in regenerative, irregular cords. Bile ducts are mildly

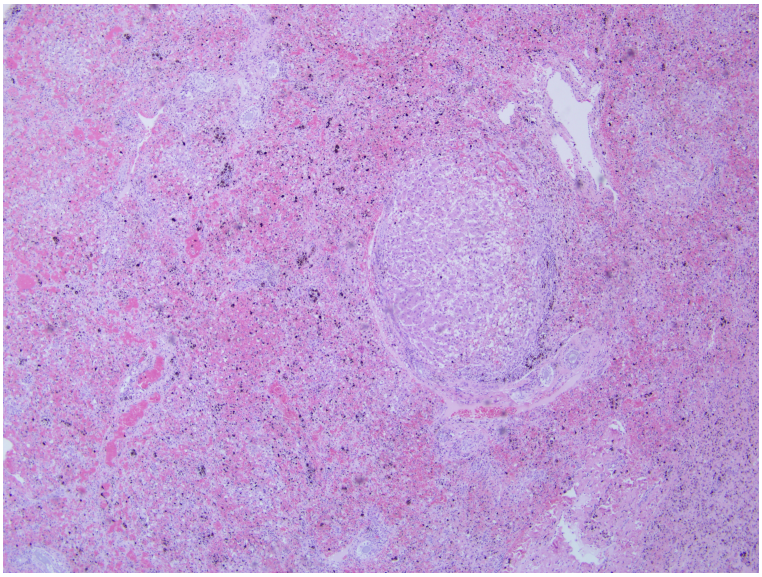

4-1. Liver, dog. Diffusely there is loss of normal hepatic parenchyma (necrosis) with multifocal islands of plump basophilic regenerative nodules. Multifocally, bile ducts and lymphatics are ectatic (HE 40X)

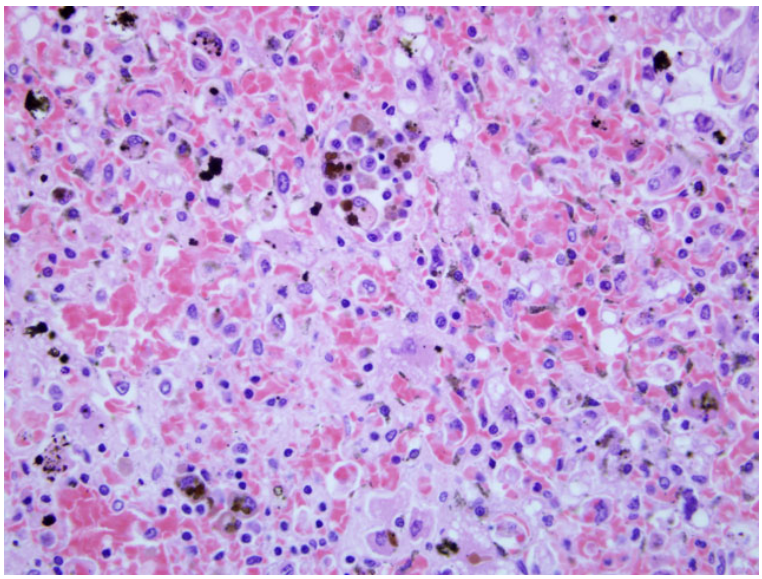

4-2. Liver, dog. Multifocally, remaining hepatocytes are discohesive with pyknotic or karyorrhectic nuclei (necrosis) or have a microvacuolated cytoplasm (lipidosis)(HE 400X)

ectatic and contain moderate amounts of pale homogenous basophilic material (bile; cholestasis). Lymphatics in the connective tissue surrounding large vessels are dilated (portal hypertension).

Contributor's Morphologic Diagnosis: Liver: Severe multifocal to coalescing subacute massive necrosis with mild cholestasis.

Contributor's Comment: The histologic finding of massive hepatic necrosis, in combination with the history of hypoglycemia, is highly suggestive of xylitol toxicity.

Xylitol is a 5-carbon sugar alcohol that occurs in small amounts as a natural intermediary during the metabolism of L-xylulose to D-xylulose.[2] It is marketed for human consumption as a sugar substitute. Profound differences exist between species in insulin secretion after administration of xylitol. In humans, rhesus monkeys, rats, and horses, the insulin release is negligible, but in dogs, rabbits, cows, goats, and baboons, insulin levels increase significantly and rapidly.[6] Xylitol's effect in cats and ferrets is unknown. In dogs, clinical signs of xylitol ingestion include vomiting, weakness, ataxia, hypoglycemia, hypokalemia, and seizures within 30 to 60 minutes of ingestion.[3]

The pathogenesis of xylitol-induced hepatic necrosis in dogs is not known, although two mechanisms have been proposed.[2] In the first proposed scenario, cellular ATP, ADP, and inorganic phosphorus reserves are depleted by intermediates of xylitol metabolism, leading to loss of membrane integrity and cell death. In the second proposed scenario, reactive oxygen species damage cellular membranes and macromolecules, leading to cell death. These proposed mechanisms are not mutually exclusive, and both, or other as yet unknown, mechanisms may be responsible.[2]

A recent paper describing the histologic lesions in two dogs exposed to xylitol described periacinar to midzonal necrosis (zones I and II) in one sample and centrilobular necrosis (zone III) in the other[2]. No zonal distribution was detected in this case, however.

The histologic picture of severe, massive hepatic necrosis is not pathognomonic, and can occur with a variety of hepatic insults, including chemicals (carbon tetrachloride), drugs (carprofen, potentiated sulfonamides), bacterial infections (*Clostridium piliformis*), and toxins (blue-green algae, Sago Palm seeds, *Amanita* mushrooms).[1,5,7,8] Anamnesis and clinicopathologic data are needed to prioritize the list of differential diagnoses.

AFIP Diagnosis: Liver: Hepatocellular degeneration, necrosis and loss, massive, subacute, diffuse, severe, with hepatocyte dissociation, hemorrhage and regeneration.

Conference Comment: The contributor provides an excellent review of xylitol toxicity in domestic species. During the conference, participants were interested in the regenerative hepatic nodules in the submitted slide. The reason for this regeneration is not evident histologically; attendees considered the possibility of concurrent pre-existent hepatic disease of a toxic nature.

The liver's ability to regenerate is intriguing and unique. The potential for hepatic regeneration depends on the viability of the hepatic stroma. Without stroma, there is no scaffolding for plate organization of new hepatocytes. Normal hepatocytes are in the G_0 resting stage of the cell cycle. Damage to the liver results in tumor necrosis factor alpha (TNF-α)-mediated activation of Kupffer cells, which then release IL-6. The effect of IL-6 on hepatocytes allows them to respond to growth factors, such as hepatocyte growth factor (HGF), transforming growth factor-α (TGFα-) and epidermal growth factor. Viable hepatocytes near the area of damage begin replicating. As restoration of the liver mass proceeds, there is increased responsiveness to growth inhibitors TGF-β and activin A. These compounds, which are downregulated during regeneration, suppress hepatocyte replication and induce extracellular matrix .[9]

Participants briefly discussed causes of hypoglycemia which fall into one of six broad categories:[4]

1. Excess insulin or insulin analogs
2. Reduced hormones that maintain glucose homeostasis
3. Reduced hepatic glycogen storage
4. Increased glucose usage
5. Reduced glucose intake or gluconeogenesis
6. Drugs

Based on the signalment, a reasonable differential diagnosis for hypoglycemia in this case would include gram-negative sepsis, malnutrition, paraneoplastic syndrome, insulinoma, or laboratory error. If the serum has prolonged contact with the blood clot in the collection tube, glucose will be depleted because of insulin-independent uptake of glucose by erythrocytes. In addition to marked hypoglycemia, hypophosphatemia, hypokalemia, hypercalcemia and increased levels of alanine aminotransferase (ALT) and aspartate aminotransferase (ASP) have been observed with xylitol intoxication in both experimental and clinical settings.[2,10]

Contributor: Department of Anatomic Pathology, Biomedical Sciences, College of Veterinary Medicine
T4 018 Veterinary Research Tower, Cornell University, Ithaca, NY 14853
http://www.vet.cornell.edu/biosci/pathology/services.cfm

References:

1. DeVries SE, Galey FD, Namikoshi M, Woo JC. Clinical and pathologic findings of blue–green algae (*Microcystis aeruginosa*) intoxication in a dog. *J Vet Diagn Invest*. 1993;5:403-408.
2. Dunayer EK, Gwaltney-Brant SM. Acute hepatic failure and coagulopathy associated with xylitol ingestion in eight dogs. *J Am Vet Med Assoc*. 2006; 229(7):1113-1117.
3. Dunayer EK. Hypoglycemia following canine ingestion of xylitol-containing gum. *Vet Hum Toxicol*. 2004;46:87-88.
4. Evans EW, Duncan JR. Proteins, lipids and carbohydrates. In: Latimer KS, Mahaffey EA, Prasse KW, eds. *Duncan and Prasse's Veterinary Laboratory Medicine: Clinical Pathology*. 4th ed. Ames, IA: Blackwell Publishing; 2003:181-187.
5. MacPhail CM, Lappin MR, Meyer DJ, et al. Hepatocellular toxicosis associated with administration of carprofen in 21 dogs. *J Am Vet Med Assoc*. 1998;212(12):1895-1901.
6. Piscitelli CM, Dunayer EK, Aumann M. Xylitol toxicity in dogs. *Compendium* 2010. E1-E4.
7. Puschner B, Rose HH, Filigenzi MS. Diagnosis of amanita toxicosis in a dog with acute hepatic necrosis. *J Vet Diagn Invest*. 2007;19(3):312-7.
8. Senior DF, Sundlof SF, Buergelt CD, et al: Cycad intoxication in the dog. *J Am Anim Hosp Assoc*. 1985;21:103-109.
9. Stalker MJ, Hayes MA. Liver and biliary system. In: Maxie MG, ed. *Jubb, Kennedy and Palmer's Pathology of Domestic Animals*. 5th ed., vol. 2. Philadelphia, PA: Elsevier Ltd; 2007:324-325.
10. Xia Z, He Y, Yu J. Experimental acute toxicity of xylitol in dogs. *J Vet Pharmacol Ther*. 2009;32:465-469.